JOURNAL OF Materials CHEMISTRY

Al_2O_3 thin films from aluminium dimethylisopropoxide by metal–organic chemical vapour deposition

Davide Barreca,[a] Giovanni A. Battiston,*[b] Rosalba Gerbasi[b] and Eugenio Tondello[a]

[a]*Dipartimento di Chimica Inorganica, Metallorganica ed Analitica - Università di Padova, Via Loredan, 4 - 35131 Padova, Italy*
[b]*Istituto di Chimica e Tecnologie Inorganiche e dei Materiali Avanzati del C.N.R. - Corso Stati Uniti, 4 - 35127 Padova, Italy. E-mail: g.a.battiston@ictr.pd.cnr.it*

Received 13th April 2000, Accepted 15th June 2000
Published on the Web 7th August 2000

This paper focuses on the use of aluminium dimethylisopropoxide as a novel precursor for the chemical vapour deposition of alumina thin films. The fragmentation pattern of this compound was studied by mass spectrometry, while its volatility and decomposition route were analysed by in-line FT-IR spectroscopy. Aluminium oxide films were grown in the temperature range 540–600 °C at a total pressure of 100 Pa in a nitrogen–oxygen atmosphere. A kinetic model was developed which includes an overall heterogeneous reaction and a parasitic one in the gas phase with apparent activation energies of 130 kJ mol^{-1} and 209 kJ mol^{-1} respectively. The microstructure, composition and morphology of the obtained layers were analysed respectively by X-ray diffraction, X-ray photoelectron spectroscopy and atomic force microscopy. The aluminium oxide films obtained were transparent, amorphous, stoichiometric, carbon-free and smooth. An island growth was proposed. Uniform growth rates along the reactor of 16, 32 and 57 nm min^{-1} are found at deposition temperatures in the range of 560–570 °C, at precursor evaporation temperatures of 15, 25 and 35 °C respectively.

Introduction

Metal oxides represent a very important group of coating materials due to their mechanical and chemical stability as well as their wide range of useful refractive indices. Aluminium oxide films offer, in principle, great potential in a large number of applications such as insulating layers, optical filters, wear resistant coatings and corrosion protective coatings;[1–4] they may be used in semiconductor device applications as a passivating layer because of their impermeability to the diffusion of alkaline ions and other impurities, or when a high dielectric constant is needed.

Chemical vapour deposition (CVD) of alumina thin films can be carried out by using different derivatives of aluminium as precursors. However the use of a highly volatile non-pyrophoric liquid precursor is advisable to make the whole process more controllable and safer. Dialkylaluminium acetylacetonates were used in a recent work but gave rise to carbon contamination in the films.[5]

Metal alkoxides have become widely used precursors in the chemical vapour deposition of oxide thin films; they are easy to prepare and purify and being intrinsically non-corrosive they can be stored almost indefinitely when kept in a dry atmosphere. A number of metal alkoxides having industrial applications are commercially available with high purity and relatively low prices. Despite these factors the use of dialkylaluminium alkoxides has until now received little attention for the deposition of Al_2O_3 thin films. The only paper on this topic[6] however, indicates aluminium dimethylisopropoxide as a non-pyrophoric liquid precursor particularly suitable for practical applications.

Experimental

Aluminium dimethylisopropoxide was synthesized[6] starting from $Al(O^iC_3H_7)_3$ and $Al(CH_3)_3$ (Aldrich). All solvents were dried and distilled under nitrogen before use. All manipulations were carried out in a dry-box.

The depositions were achieved in a low-pressure hot wall reactor described elsewhere,[7] equipped with an in-line FT-IR spectrometer to monitor exhaust gases. The reactor was provided with a Pyrex pipe, inner diameter 4.8 cm, 31 cm long. Nitrogen (20 sccm) was employed as carrier gas and oxygen (50 sccm) as reactant gas, keeping the whole system at a total pressure of 100 Pa. The temperature of the decomposition zone was monitored by a thermocouple placed in a fixed position in the reactor tube; a previous calibration enabled us to know the temperature profile in the reactor through an analytical relationship between position and the thermocouple temperature.[7]

Aluminium oxide films were grown in the temperature range 540–600 °C; the thickness in the range 200–1200 nm, and refraction index of alumina films were measured by interference fringe analysis as reported elsewhere.[8]

Soda-lime glass substrates were cleaned prior to introduction into the reactor; they were immersed in soaped water, washed with distilled water and rinsed in isopropyl alcohol. After repeating this procedure ten times, the substrates were dried in air.

The FT-IR data were collected by an ATI Mattson Genesis Series instrument with an MCT detector used in the range 4000–400 cm^{-1} with 4 cm^{-1} resolution.

Diffraction patterns were collected by an instrument based on a standard Philips 1830 generator, an optically encoded PW 3020 goniometer and a sealed tube with copper anode.

Atomic force microscopy (AFM) was performed using a Park Autoprobe CP instrument operating in contact mode in air. The background was subtracted from the images using the ProScan 1.3 software from Park Scientific (Sunnyvale, CA, USA).

A Perkin Elmer Φ 5600ci spectrometer with Al-Kα radiation (1486.6 eV) was used for the X-ray photoelectron spectroscopy (XPS) analyses. The working pressure was less than 1.8×10^{-9} mbar. The spectrometer was calibrated by assuming the binding energy (BE) of the Au $4f_{7/2}$ line at 83.9 eV with respect to the Fermi level. After a Shirley-type background subtraction, the raw spectra were fitted using a non-linear least-squares fitting program adopting Gaussian–Lorentzian shapes

DOI: 10.1039/b002968h

for all the peaks. The atomic compositions were evaluated using sensitivity factors as provided by Φ V5.4A software (Perkin Elmer, Physical Electronics, Eden Prairie, MN, USA). Ar^+ sputtering was carried out at 2.5 kV, 0.4 μA cm^{-2} beam current density with an argon partial pressure of 4×10^{-8} mbar.

Results and discussion

Preliminary mass spectrometry studies have given some clues on the thermal stability and fragmentation of the precursor $Al(CH_3)_2(O^iC_3H_7)$. The molecular ion is dominant ($m/z = 116$), and two main routes of fragmentation could be envisaged, finally obtaining the $[Al–O]^+$ ($m/z = 43$, 57%) and $[AlH]^+$ ($m/z = 28$, 25%) species respectively. The absence of carbide species and the elimination of organic ligands suggests a good possibility of an MOCVD utilisation of this compound with a low carbon contamination in the films. Nevertheless the presence of the molecular ion at $m/z = 116$ as the dominant species shows that the molecule is relatively stable.

Gas phase composition in the MOCVD reactor was preliminarily studied by FT-IR spectroscopy using a cell in line to the reactor tube, varying the reactor temperature in the range 100–600 °C and keeping the precursor bath temperature at 25 °C.

In Fig. 1 the measured spectra at different reactor temperatures are reported. The typical IR spectrum of $Al(CH_3)_2(O^iC_3H_7)$ is shown at a temperature of 100 °C: in the high wavenumber region only typical C–H stretching bands at 3060–2857 cm^{-1} are present, in the medium region we can observe the following bands: 1390 cm^{-1} CH_3 bending, 1200 cm^{-1} CH_3 bending, 1128 cm^{-1} C–O stretching, 968 cm^{-1} C–C stretching, 835 cm^{-1} CH_3 rocking, 705 cm^{-1} Al–O and Al–C stretching bands.[9] On increasing the reactor temperature, no appreciable effect on the IR spectrum is observed up to 500 °C, while the band intensities became weaker at 540 °C and eventually quite undetectable at 580 °C. There results are an important starting-point to establish the useful temperature range for film deposition.

The precursor evaporation rate *versus* precursor bath temperature in the range 15–35 °C was analytically determined through IR absorbance measurements, by means of the Beer–Lambert law, with the MOCVD reactor kept at a temperature of 100 °C. The molar absorption coefficient at each wavenumber was previously obtained by estimating the evaporation rate as weight loss at the bath temperature of 25 °C. The Clausius–Clapeyron-like relationship between the precursor evaporation rate (mol min^{-1}) and the bath temperature T_b (K) is obtained as

$$\ln(\text{precursor evaporation rate}) = 14.549 - 6532/T_b \quad (1)$$

through a logarithmic plot of the evaporation rate *vs.* $1/T_b$ in a stationary situation that gives a straight line with a regression coefficient of 0.998 (Fig. 2).

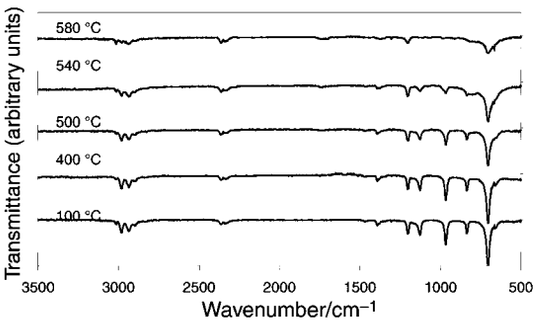

Fig. 1 FT-IR gas phase transmittance spectra at the reported reactor temperatures.

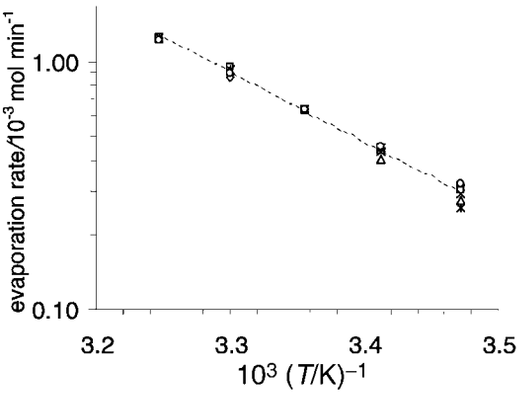

Fig. 2 Evaporation rate for $(CH_3)_2AlO^iPr$ as a function of temperature. Symbols refer to vibrational bands, dotted line to the least squares regression.

This relation is useful to establish how to vary the entrance precursor concentration; in the following when not otherwise specified, the bath temperature is kept at 25 °C.

A kinetics study of thin film growth was performed on the basis of an overall heterogeneous surface reaction, intrinsic for the alumina growth, and a parasitic reaction in the gas phase representing many possible decomposition reactions ineffective for the film deposition. These reactions could span from the formation of adducts between decomposition products and precursor[10] to the nucleation in the gas phase of aluminium oxide hydrates leading to the formation of powders. In particular both the water, normally formed during the decomposition process of alkoxide precursors,[11] and oxygen could act as nucleation centres in the gas phase or on the substrate surface as well as larger particulates;[12] little is reported in the literature but this nucleation could have an important role for a complete assessment of the precursor consumption.

Fig. 3 shows the variation of the Al_2O_3 deposition rate at different reactor temperatures as a function of the axial reactor co-ordinate. The deposition rate increased with temperature suggesting a chemical kinetics controlled domain. We assumed that the reaction rate depended only on the precursor concentration, because oxygen was in large stoichiometric excess, so pseudo first-order kinetics were used. The analysis was carried out only in the axial reactor dimension on the basis of the high uniformity of film thickness in the radial direction. The equation of precursor mass continuity can be expressed along the reactor as:

$$\frac{\partial c}{\partial x} = -(k^{\text{film}} + k^{\text{pwd}}) \cdot c/v \quad (2)$$

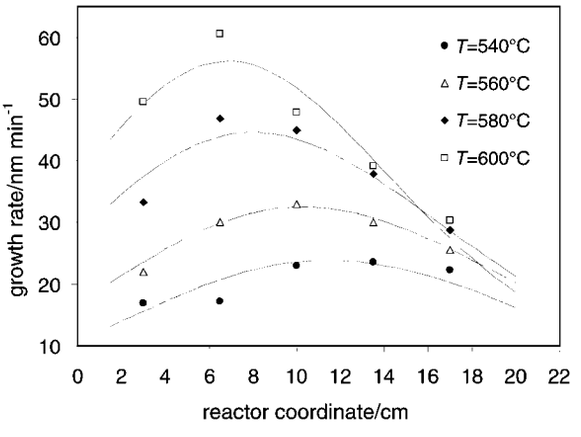

Fig. 3 Growth rate at the reported temperatures as a function of axial reactor co-ordinate. Symbols represent experimental data, lines the calculated trends.

where $k^{film} = k_0^{film}\exp(-E^{film}/RT)$ represents the chemical kinetics trend of film formation, $k^{pwd} = k_0^{pwd}\exp(-E^{pwd}/RT)$ is related to the parasitic powdering, c is the concentration of precursor in mol cm^{-3}, k_0^{film} and k_0^{pwd} are pre-exponential factors in min^{-1}, E^{film} and E^{pwd} are the apparent activation energies, x is the axial co-ordinate in cm and v is the linear velocity of the gaseous mixture in cm min^{-1} depending on reactor temperature and pressure, and to a lesser extent, on the precursor feed through its evaporation rate.

Eqn. (2) cannot be analytically solved because the temperature, and consequently v, is a function of x, as explained in the experimental part. The variation of the temperature along the reactor tube has to be carefully considered, since only this explains why at the beginning of the tube, where the precursor concentration is at a maximum but not the temperature value, the corresponding growth rate is not yet at the maximum value.

We can consider the reactor pipe divided into a number of finite elements or boxes, where the temperature can reasonably be assumed constant. For the n^{th} box the entrance precursor concentration $c_{n(0)}$ corresponds to the concentration exiting from the $n-1^{th}$ box; in particular for the first box the entry $c_{1(0)}$ is obtained by dividing the evaporation rate from eqn. (1) by the total flux. The solution of eqn. (2) inside the n^{th} box can be easily obtained as:

$$c_n = c_{n(0)} \cdot e^{-k^{film} \cdot x/v} \cdot e^{-k^{pwd} \cdot x/v} \quad (3)$$

and consequently the growth rate r_n is obtained as:

$$r_n = \left(\frac{dh}{dt}\right)_n = c_n \cdot L \cdot k^{film} \cdot \frac{W_{Al_2O_3}/2}{\rho} \quad (4)$$

where h is the thickness of the film, ρ is the alumina density, $W_{Al_2O_3}$ is the molecular weight of Al_2O_3 and L is the ratio between the reactor volume and the reactive area and set equal to 1 cm.

The reaction parameters k_0^{film}, k_0^{pwd}, E^{film} and E^{pwd} were determined by matching both eqn. (3) with the precursor concentration at the end of the reactor evaluated by FT-IR measurements, and eqn. (4) with the experimental growth rates as a function of reactor temperature and position along the reactor (see Fig. 3).

The values of E^{film}, k_0^{film}, E^{pwd} and k_0^{pwd} resulted as: 130 kJ mol^{-1}, 2×10^{10} min^{-1}, 209 kJ mol^{-1} and 4×10^{15} min^{-1} respectively. The value of E^{film} found was comparable to others obtained for TiO_2 or ZrO_2 films starting from alkoxide derivatives, *e.g.* 126 kJ mol^{-1} and 127 kJ mol^{-1} for $Ti(O^iC_3H_7)_4$ and $Zr(O^tC_4H_9)_4$ respectively.[7,13] This analogy suggests that the behaviour of the precursor aluminium dimethylisopropoxide be determined by the alkoxide moiety.

For an industrial production, uniform and high growth rates

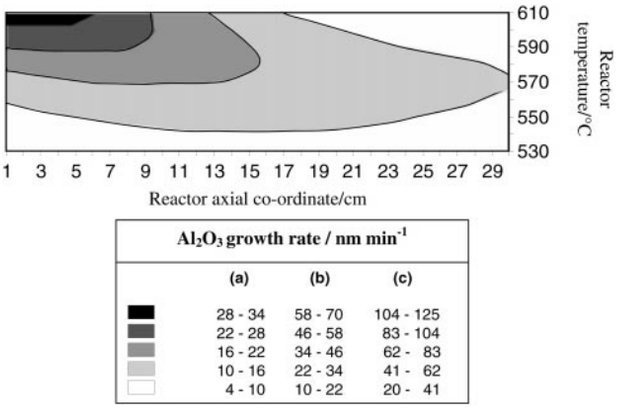

Fig. 4 Contour lines simulation of growth rate along the reactor as a function of reactor temperature. The growth rate values reported in the legend depend on the precursor temperatures of 15, 25 and 35 °C, corresponding to (a), (b) and (c) respectively.

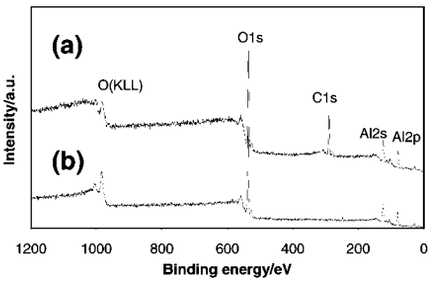

Fig. 5 XPS surveys of an alumina film on a lime-glass substrate as grown at 560 °C (a), and after 15 minutes argon sputtering (b).

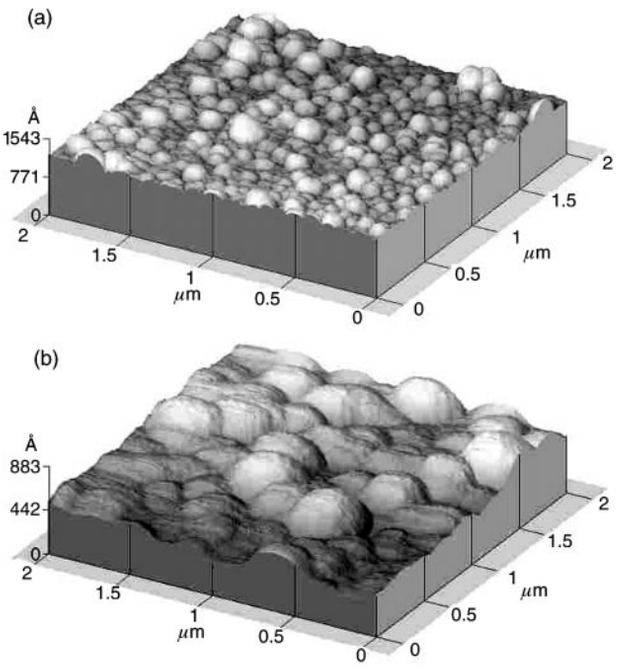

Fig. 6 AFM 3D images of alumina films grown at 560 °C for 7 minutes (a) and 20 minutes (b).

along the reactor are required. A contour lines plot of the growth rate as a function of reactor temperature and reactor co-ordinate is reported in Fig. 4. An increase of the precursor evaporation rate, obtained by varying the bath temperature in the range 15–35 °C, gave rise to a substantially linear increase in the growth rate; this effect is shown in the legend of Fig. 4. It can be concluded that quite uniform growth rates were obtained at reactor temperatures of 560–570 °C; the mean growth rates in this range were 16, 32 and 57 nm min^{-1} with a standard deviation of 6%, for precursor evaporation temperatures of 15, 25 and 35 °C respectively.

All the obtained films were transparent and amorphous by X-ray diffraction analysis.

The chemical composition of the films was studied by XPS. Fig. 5 reports the surveys recorded for an as-grown Al_2O_3 film on soda-lime glass at 560 °C. The surface spectrum (Fig. 5(a)) showed the presence of carbon, oxygen and aluminium as the only surface elements. No other signals were detected, indicating a uniform coverage of the substrate. The presence of aluminium oxide was confirmed by the BE of the Al 2p peak, the value of which (74.0 eV) is in good agreement with literature data.[14] Further indications came from the O/Al atom ratio, which was close to the theoretical value (1.5), and from the O 1s BE (531.0 eV), which was close to the data reported for Al_2O_3.

Fig. 5(b) shows the survey spectrum for the same sample after 15 minute sputtering. As can be noted, the carbon signal is now below the XPS detection limits. This effect proves that the

presence of carbon on the film surface was caused by atmospheric contamination and was not due to carbonaceous fragments arising from the alkyl moieties of the precursor. Therefore the obtained films were carbon free and the precursor had a clean decomposition pattern.

AFM micrographs for the obtained films showed the presence of a fine texture, with globular grains well interconnected between themselves (see Fig. 6(a),(b) for samples grown at 560 °C for 7 min and 20 min respectively). The obtained average roughness fell in the range 5–6 nm. A striking difference between the two samples of Fig. 6 was given by the average grain dimensions. In fact, on going from 7 to 20 minutes we observed an increase of film grain size from about 90 to 300 nm.

Since the surface morphology and grain shapes did not show other marked changes, we are left to suppose that in our running conditions film growth occurred by a "Volmer–Weber" or "island" mode,[15] where the island sizes became gradually bigger for higher deposition times. This hypothesis was supported by the absence of preferential orientation in the crystalline microstructure (the films were amorphous) and the observation of a surface reaction regime in the temperature range studied.

Conclusions

In this work the growth of Al_2O_3 films in a low-pressure hot wall MOCVD system is discussed using aluminium dimethyl-isopropoxide as precursor. This compound whose synthesis, mass analysis, evaporation rate and decomposition were exploited, is shown to be a promising precursor, especially because of its high volatility, easy synthesis and purification, and eventually low cost.

A kinetic model involving an intrinsic reaction of Al_2O_3 deposition and a parasitic powdering reaction was found to fit the experimental results quantitatively over a large temperature range. According to the model, uniform and high growth rates along the reactor were estimated in the deposition temperature range 560–570 °C.

Since the Al_2O_3 films obtained in this study were transparent, amorphous, smooth and free of contaminants, they appear to be valuable candidates for a wide range of industrial applications.

Acknowledgements

The authors are indebted to Dr U. Vettori for mass analysis in the facilities of CNR-Centro Studio Stabilità e Reattività Composti Coordinazione in Padova.

References

1 B. Lux, C. Colombier, H. Altena and K. Stjernberg, *Thin Solid Films*, 1986, **138**, 49.
2 J. S. Kim, H. A. Marzouk, P. J. Reucroft, J. D. Robertson and C. E. Hamrin Jr., *Appl. Phys. Lett.*, 1993, **62**, 681.
3 V. A. C. Haanappel, J. B. Rem, H. D. van Corbach, T. Fransen and P. J. Gellings, *Surf. Coat. Technol.*, 1995, **72**, 1.
4 V. A. C. Haanappel, D. V. D. Vendel, H. S. C. Metselaar, H. D. van Corbach, T. Fransen and P. J. Gellings, *Thin Solid Films*, 1995, **254**, 153.
5 G. A. Battiston, G. Carta, R. Gerbasi, M. Porchia, L. Rizzo and G. Rossetto, *J. Phys. IV*, 1999, **9**, 675.
6 W. Koh, S.-J. Ku and Y. Kim, *Thin Solid Films*, 1997, **304**, 222 and references therein.
7 G. A. Battiston, R. Gerbasi, M. Porchia and A. Gasparotto, *Chem. Vap. Deposit.*, 1999, **5**, 13.
8 R. Swanepoel, *J. Phys. E: Sci. Instrum.*, 1983, **16**, 1214.
9 D. C. Bradley, R. C. Mehrotra and D. P. Gaur, in *Metal Alkoxides*, Academic Press, London–New York–San Francisco, 1978.
10 H. Gris, B. Caussat, H. Vergnes and J. P. Couderc, *Electrochem. Soc. Proc.*, 1997, **25**, 194.
11 G. A. Battiston, R. Gerbasi, M. Porchia and A. Marigo, *Thin Solid Films*, 1994, **239**, 186.
12 W. L. Gladfelter, *Chem. Mater.*, 1993, **5**, 1372.
13 P. Stocco, Thesis, Padua University, 1999.
14 J. F. Moulder, W. F. Stickle, P. E. Sobol and K. D. Bomben, *Handbook of X-Ray Photoelectron Spectroscopy*, ed. J. Chastain, Perkin Elmer Corporation, Eden Prairie, MN, USA, 1992.
15 T. J. Spencer, *Progr. Inorg. Chem.*, 1994, **41**, 145.